

## Supporting Information

### The Acute Immune Response of Micro- and Nanosized Erythrocyte-Derived Optical Particles in Healthy Mice

Taylor M. Hanley, Raviraj Vankayala, Jenny T. Mac, David D. Lo, and Bahman Anvari\*

**Characterization of NETs.** As determined by fitting Lognormal distributions to the dynamic light scattering-based estimates of hydrodynamic diameters, the mean peak diameters ( $\pm$  standard deviation (SD)) of the various types of NETs were as follows:  $2,738 \pm 26$  nm for  $\mu$ NETs,  $109.26 \pm 0.592$  nm for nNETs,  $91.376 \pm 0.879$  nm for FF-nNETs, and  $106.81 \pm 0.93$  nm for HF-nNETs (Figures S1a, b). The mean  $\pm$  SD values of zeta potentials for the particles were as follows:  $-14.72 \pm 1.32$  mV for  $\mu$ NETs,  $-14.16 \pm 0.77$  mV for nNETs,  $-11.86 \pm 0.56$  mV for FF-nNETs, and  $-15.08 \pm 0.59$  mV for HF-nNETs (Figure S1c). FF-nNETs had a significantly higher zeta potential than all the other particles ( $p < 0.01$  for all comparisons), and nNETs had a significantly higher zeta potential than HF-nNETs ( $p < 0.05$ ).

In response to photo-excitation at  $720 \pm 2.5$  nm, all particle types produced similar fluorescence emission spectra (Figure S1d). The peak normalized fluorescence emission intensity at  $\approx 800$  nm is associated with the monomer form of ICG. These results suggest that the diameter and the functionalization agent did not affect the fluorescence of the particles. After incubation with the Goat Anti-Human IgG FITC-labeled antibody, the HF-nNETs showed an emission peak at  $\approx 525$  nm (Figure S1e) in response to photo-excitation at  $488 \pm 2.5$  nm, confirming the conjugation of Herceptin® onto NETs.

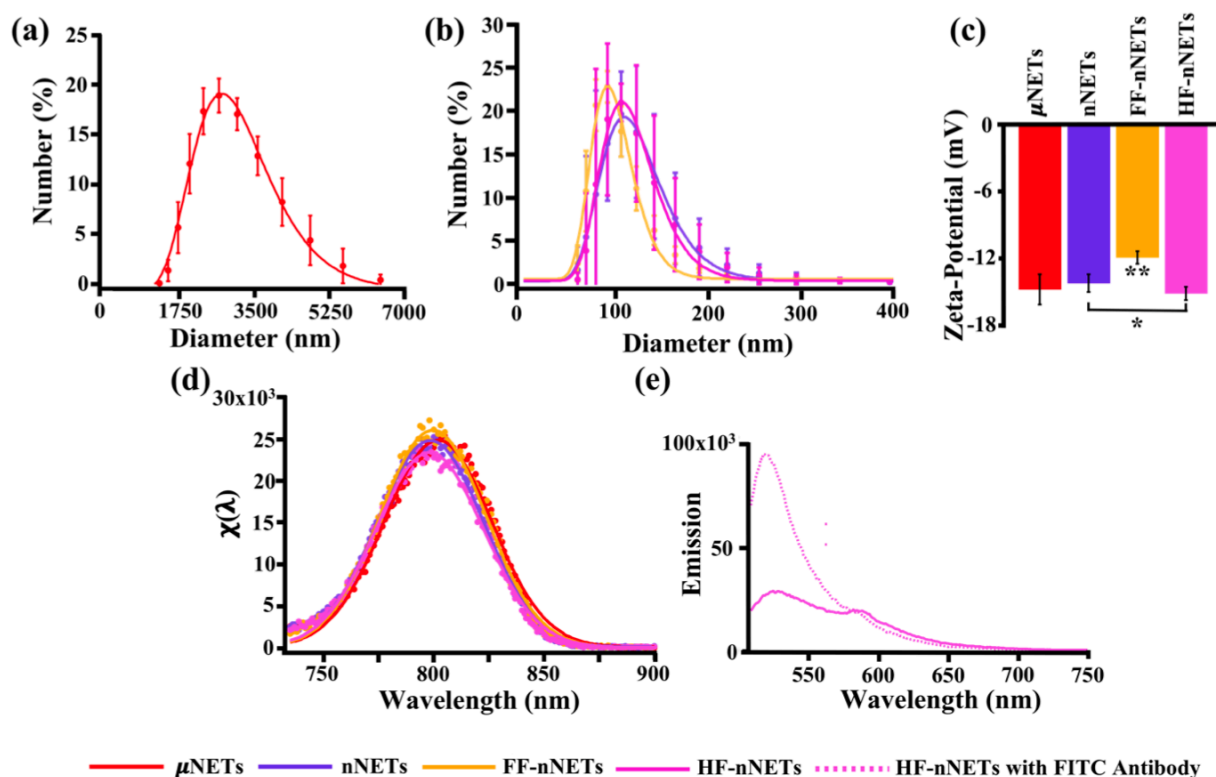


**Figure S1.** Characterization of the various types of NETs. Hydrodynamic diameters of (a)  $\mu$ NETs and (b) nNETs, FF-nNETs, and HF-nNETs as measured by dynamic light scattering. We present the average (circles) of three measurements made on each sample. Error bars are standard deviations from the average values. LogNormal fits to the measured data are shown as solid traces. (c) Zeta potentials for all particle types in 1xPBS ( $\approx 320$  mOsm phosphate buffer saline). Average of five measurements (bars) with standard deviation (error bars) for each sample are presented. Statistical significance of \* ( $p < 0.05$ ), and \*\* ( $p < 0.01$ ) are indicated. Significance markings directly above FF-nNETs indicates that the zeta potential for FF-nNETs is significantly different from those associated with the other particles at the indicated significance level. Bracket indicates that the zeta potential for nNETs and HF-nNETs are different from each other at the indicated significance level. (d) Normalized emission spectra (see equation 1 in manuscript) in response to photo-excitation at  $720 \pm 2.5$  nm for all particles in 1xPBS. Data points (circles) with Gaussian fits (solid traces) are shown. (e) Raw emission spectra in response to photo-excitation at  $488 \pm 2.5$  nm of HF-nNETs with and without incubation with FITC-labeled secondary antibody.

**Endotoxin Assessment.** We present the results of the endotoxin measurements for the three standard samples consisting of LAL grade water containing different known levels of endotoxin units (EU/ml), and 1:100 dilutions of  $\mu$ NETs and nNETs samples (Figure S2).

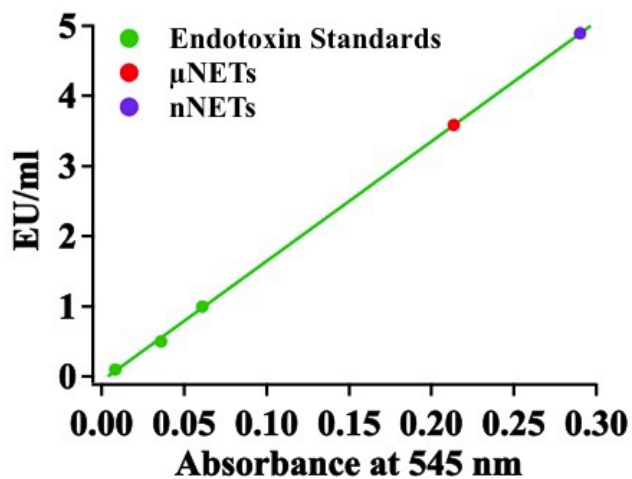


**Figure S2.** Endotoxin levels for three standard samples,  $\mu$ NETs, and nNETs. The straight line is the calibration curve fitting the standard measurements. Samples of  $\mu$ NETs and nNETs were diluted 1:100 prior to the measurements.

**Flow cytometry.** We show illustrative results associated with APC fluorescence emission associated with each of the investigated cytokines in Figure S3. Representative results for 5-parameter logistic fits to the standards corresponding to each of the cytokines are presented in Figure S4.

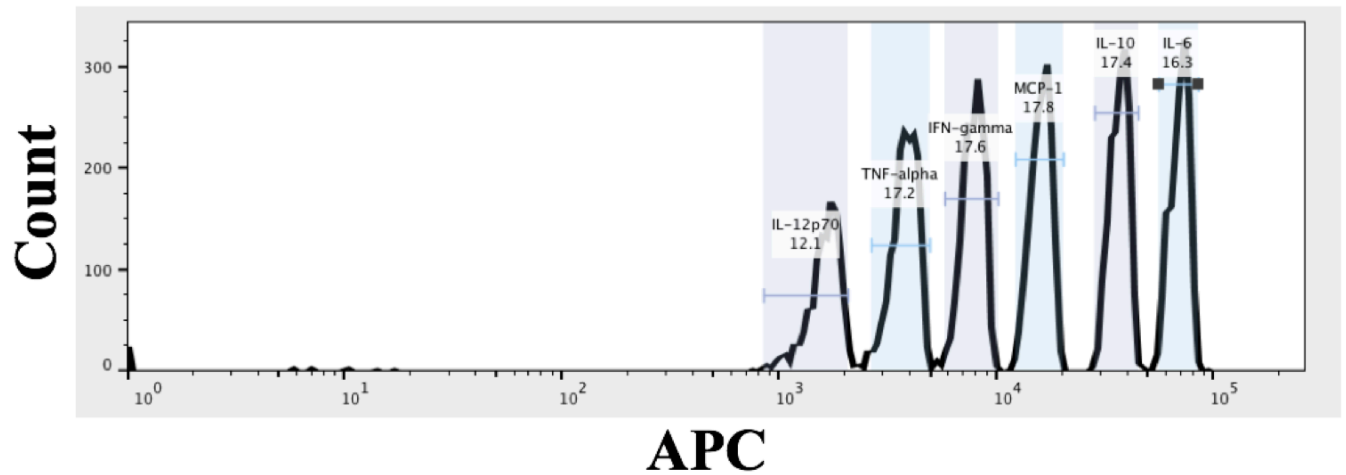


**Figure S3.** Representative bead clustering based on APC fluorescence emission for six separate bead populations corresponding to IL-12p70, TNF- $\alpha$ , IFN- $\gamma$ , MCP-1, IL-10, and IL-6. Horizontal bars indicate the range of APC fluorescence intensities associated with each cytokine bead population.

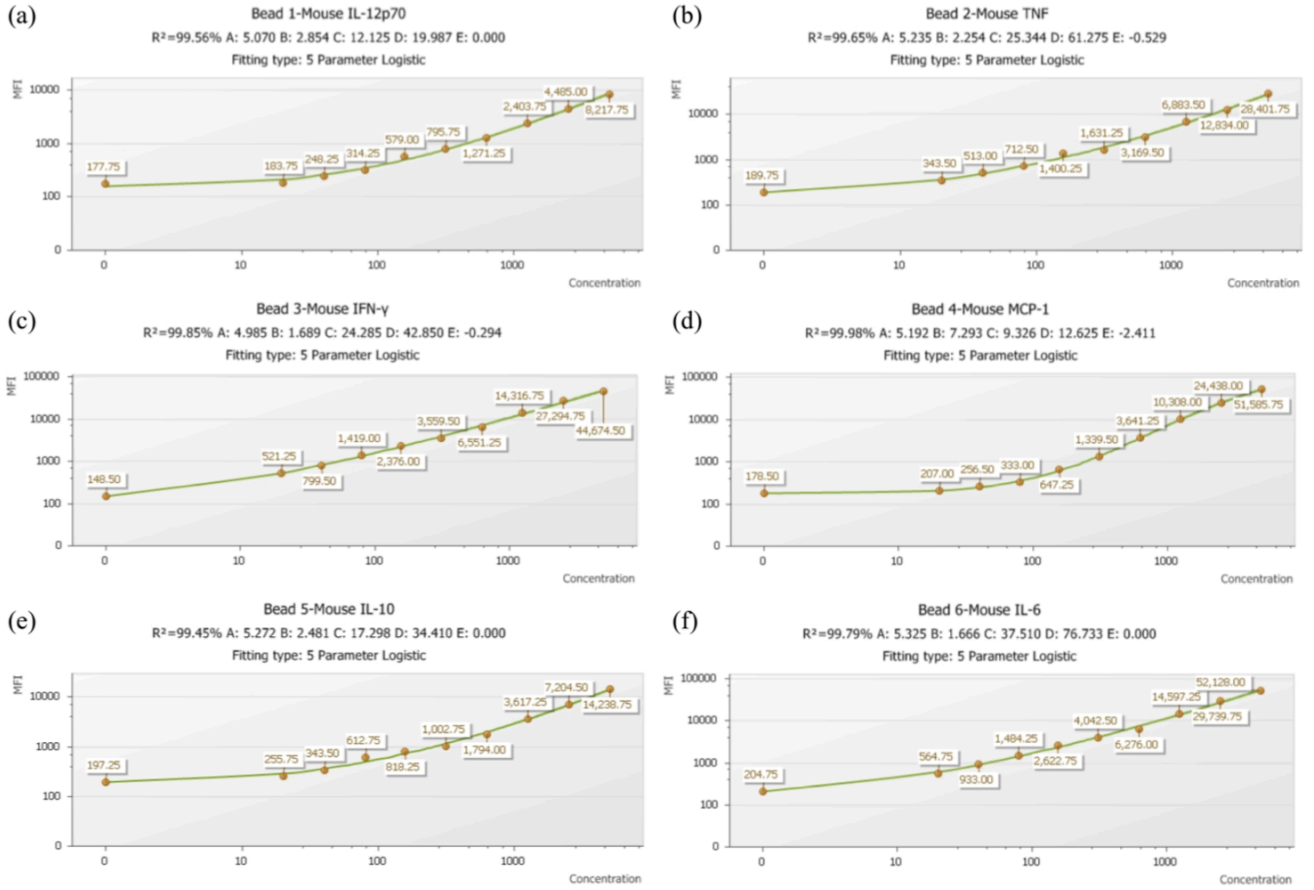


**Figure S4.** Representative 5-Parameter Logistic fits for (a) IL-12p70, (b) TNF- $\alpha$ , (c) IFN- $\gamma$ , (d) MCP-1, (e) IL-10, and (f) IL-6.